

Heavy quark potential at high temperature

Yannis Burnier

Ecole Polytechnique Fédérale de Lausanne
Switzerland

Talk based on:

[YB, A. Rothkopf, 1307.6106
YB, O. Kaczmarek, A. Rothkopf, 1410.2546]

November 13, 2014

Quarkonium 2014 CERN

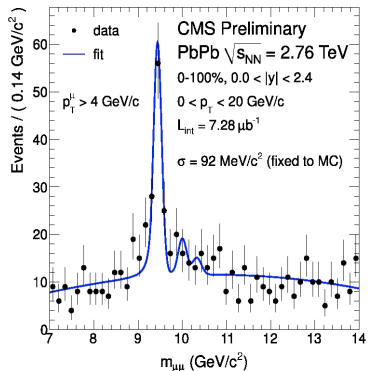
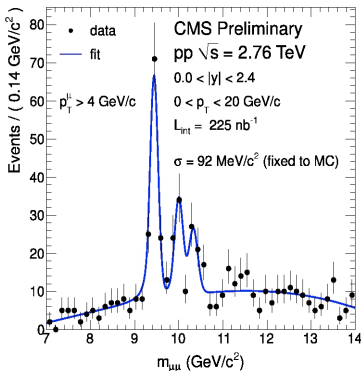
Outline

- 1 Introduction
- 2 Potential from the lattice
- 3 Results and their stability
- 4 Conclusion

Heavy quarkonium as probe for QGP

Heavy quarkonium is an important probe for quark-gluon plasma created in heavy ion collisions [T. Matsui, H. Satz (1986)].

- The disappearance of states \Leftrightarrow properties of the plasma.



[CMS, PRL 107, 052302]

- First step towards heavy ion collision: understand the properties of quarkonium in a thermal plasma.

Effective field theory description of heavy quarkonium

At $T = 0 \rightarrow$ hierarchy of scales: $M_Q \gg p = mv \gg E_{binding}$.

- Quarkonium can be described by a Schrödinger equation.
- The potential can be calculated from the Wilson loop:

$$i\partial_t W_{\square}(t, r) = \Phi(t, r) W_{\square}(t, r), \quad (1)$$

- At late times, $\Phi(t, r)$ stabilizes \leftrightarrow **static potential**:

$$V(r) = \lim_{t \rightarrow \infty} \Phi(t, r) = \lim_{t \rightarrow \infty} i \frac{\partial_t W_{\square}(t, r)}{W_{\square}(t, r)}. \quad (2)$$

At $T > 0$, if $M_Q \gg p \gg T \sim E_{binding}$, we can do the same but

$$W_{\square}(t \rightarrow \infty, r) = W_E(\tau \rightarrow it \rightarrow i\infty, r). \quad (3)$$

In HTL resummed perturbation theory, we get:

$$V(r) = -\frac{g^2 C_F}{4\pi} \left[m_D + \frac{\exp(-m_D r)}{r} + iT \phi(m_D r) \right] + \mathcal{O}(g^4).$$

[Laine, Philipsen, Romatschke, Tassler (2007); Brambilla, Ghiglieri, Vairo and Petreczky (2008); Beraudo, Blaizot, Ratti (2008)]

Potential for heavy quarks

$$V_S(r) = -\frac{g^2 C_F}{4\pi} \left[m_D + \frac{\exp(-m_D r)}{r} + iT \phi(m_D r) \right] + \mathcal{O}(g^4).$$

- First term \rightarrow 2 \times thermal mass correction for heavy quarks.
- Second term \rightarrow standard Debye-screened potential.
- Third *imaginary* term \rightarrow damping:

$$\phi(x) \equiv 2 \int_0^\infty \frac{dz z}{(z^2 + 1)^2} \left[1 - \frac{\sin(zx)}{zx} \right]$$

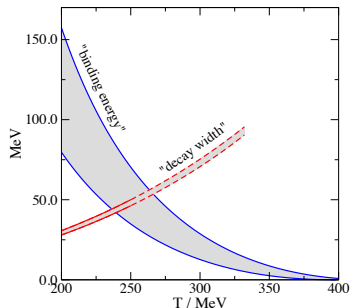
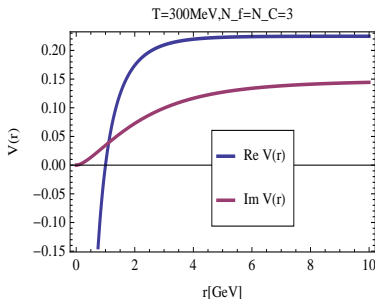
- $\phi(x)$ is strictly increasing from $\phi(0) = 0$, $\phi(\infty) = 1$.
- $r \rightarrow \infty$ contribution, 2 \times single quark damping (quark absorption in the plasma).
- Destructive interference between the dampings.

The solution for the Schrödinger equation in real time decays \rightarrow loss of correlation between initial and final state \rightarrow [decoherence](#).

Effective field theory picture of quarkonium melting

Increasing the temperature:

- The binding energy (from $\text{Re}V$) decreases.
- The decay width (from $\text{Im}V$) increases.



- When curves meet quarkonium melts [Laine, Philipsen, Romatschke, Tassler 2006].
- $\text{Im}V \propto T$ and not $m'_D(T)$ but hard to thrust HTL close to T_C .

Potential from the lattice

In Euclidean lattice simulations:

- It is easy to measure $W_{\square}(r, \tau)$ at each points of the lattice.
- It is much harder to perform the limit $\tau \rightarrow it \rightarrow i\infty!$

We should find another way...

- Let's restart from the Schrödinger equation.

$$i\partial_t W_{\square}(t, r) = \Phi(t, r)W_{\square}(t, r), \quad (4)$$

- Look for other consequence of the existence of the **potential description**:

$$\Phi(r, t) = V(r) + \phi(r, t) \quad \text{with} \quad \lim_{t \rightarrow \infty} \phi(r, t) = 0. \quad (5)$$

Consequences of the potential description

The Schrödinger equation can be solved:

$$W_{\square}(r, t) = \exp[-i(\operatorname{Re}\mathbf{V}(r)t + \operatorname{Re}\sigma(r, t)) - |\operatorname{Im}\mathbf{V}(r)|t + \operatorname{Im}\sigma(r, t)],$$

where $\sigma(r, t) = \int_0^t \phi(r, t) dt$.

Perform Fourier transform and use $W(r, -t) = W^*(r, t)$:

$$\rho_{\square}(r, \omega) = \frac{1}{2\pi} \int_{-\infty}^{\infty} dt \exp[i(\omega - \operatorname{Re}\mathbf{V}(r))t - i\operatorname{Re}\sigma(r, |t|)\operatorname{sign}(t) - |\operatorname{Im}\mathbf{V}(r)||t| + \operatorname{Im}\sigma(r, |t|)]. \quad (6)$$

From this expression, the **short time physics** $\phi(r, t)$, that vanishes at some t_{∞} can be separated from the **large time physics** $V(r)$.

Consequences of the potential description

- The late time physics can be integrated analytically.
- Short time physics can be expanded supposing that $(\text{Re}V(r) - \omega)t_\infty$ is small:

$$\rho_\square(r, \omega) \propto \frac{|\text{Im}V(r)|\cos[\text{Re}\sigma_\infty(r)] - (\text{Re}V(r) - \omega)\sin[\text{Re}\sigma_\infty(r)]}{\text{Im}V(r)^2 + (\text{Re}V(r) - \omega)^2} + c_0(r) + c_1(r)(\text{Re}V(r) - \omega) + \dots \quad (7)$$

where $\sigma_\infty(r) = \sigma(r, \infty)$. [YB, Rothkopf 2012]

- $\rho(r, \omega)$ contains a skewed Breit-Wigner peak.
- We only need to fit this lowest lying peak to get $V(r)$.
- Same statement holds for $W_{||}(r, t)$ in Coulomb gauge
 - In HTL perturbation theory $\text{Re}V, \text{Im}V, \sigma_\infty$ are the same.
- Earlier studies [Rothkopf, Hatsuda, Sasaki 2011] used a Lorentzian.

Importance of skewing

We can use HTL perturbation theory to make a test of the method:

We know $V(r)$ and calculate $C_E(r, \tau)$, $C_>(r, t)$, $\Phi(r, t)$, $\rho(r, \omega) \dots$

Parameters: $e^{\text{Im}\sigma_\infty(r)}$, $\text{Im}V(r)$, $\text{Re}V(r)$; $\text{Re}\sigma_\infty(r)$; $c_0(r)$; $c_1(r)$; $c_2(r)$.

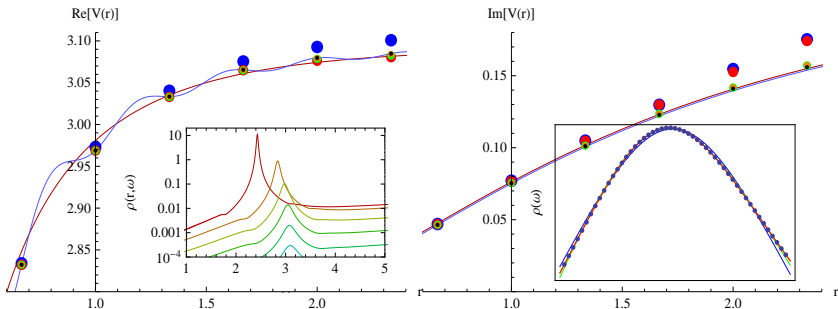
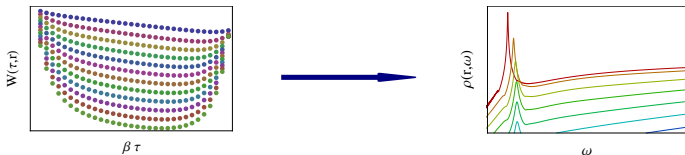


Figure: Re and Im part of the potential from different fits (units: GeV, red line: continuum potential, blue line: potential with UV cutoff).

The lowest peak contains all the information for the potential!

Can we get the spectral function?

We can get the potential from the spectral function but still lattice provides us only Euclidean correlators:



The aim is to invert an integral equation of the form

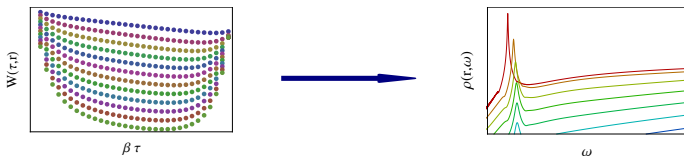
$$W(\tau) = \int d\omega K(\omega, \tau) \rho(\omega), \quad (\text{here } K(\omega, \tau) = e^{-\omega\tau}) \quad (8)$$

i.e get $\rho(\omega)$ with N_τ points $D_n = W(\tau_n)$ known to some accuracy.

- Discretize frequency space with n_ω points spaced by $\Delta\omega_l$.
- Denoting $\rho(\omega_l) = \rho_l$, $l = 1..n_\omega$, equation (8) becomes

$$D_i^p = \sum_{l=1}^{n_\omega} \Delta\omega_l K_{il} \rho_l. \quad (9)$$

Difficulties in the analytical continuation



From the discretized version:

$$D_i^p = \sum_{l=1}^{n_\omega} \Delta\omega_l K_{il} \rho_l. \quad (10)$$

It looks like we just have to **invert the matrix $\Delta\omega_l K_{il}$** . However:

- The data contains errors $\rightarrow \rho_l$'s not completely fixed.
- The spectrum contains sharp peaks, whose shape is of interest \rightarrow fine discretization needed for ω so that $n_\omega \gg N_\tau$.

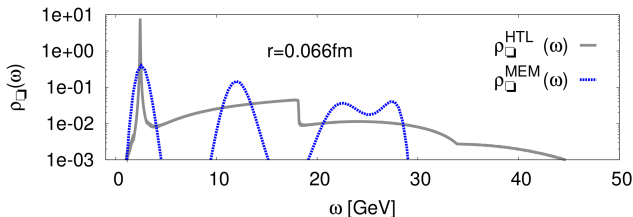
Maximum Entropy Method

The inversion can be made unique:

- Require the solution to minimize the distance to a prior m .
- The distance is defined by an entropy functional $S(\rho, m)$.

Common: usual or extended **MEM** [Asakawa et al 2003, Rothkopf 2011].

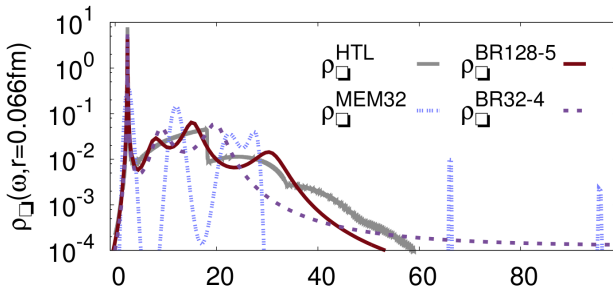
- It can't resolve the width of the peak [YB,Rothkopf 2013].
- The peak does not have a Lorentzian shape.
- Marginal improvements with better data.
- Numerically too expensive to deal with very good data.



New Bayesian reconstruction (BR) method:

We derived a **new Bayesian method** solving problems of MEM.

- All points ρ_l are **degrees of freedom**.
 - MEM has N_T d.o.f., Extended MEM can have $\sim 10^2$.
 - BR can have 10^4 and we can place them as we want.
- New **Entropy S** functional without flat directions.
- Hyperparameters integrated explicitly (**no Gaussian approximation**).



Here the prior m was set to a constant [YB, Rothkopf (2013)].

Quenched Lattice

We generated new **quenched anisotropic** ($\xi = 3.5, \beta = 7$) lattice data of size $32^3 \times N_\tau$ with $N_\tau = 24, 32, 40, 48, 56, 64, 72, 80, 96$ corresponding to $T = 839..209 \text{ MeV}$.

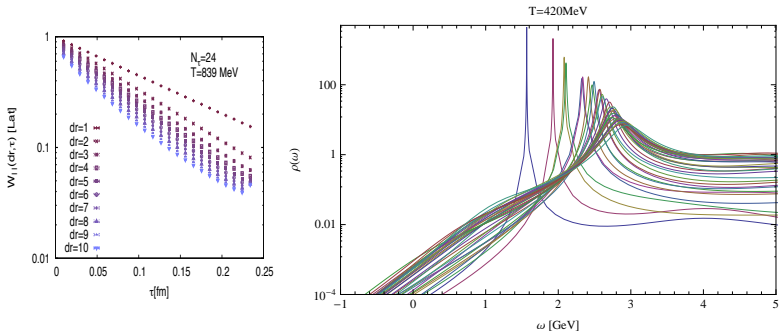


Figure: Spectrum for $1.56 T_c$

Temperature dependence of the potential: Quenched Lattice

Real and Imaginary part of the potential at different temperature.

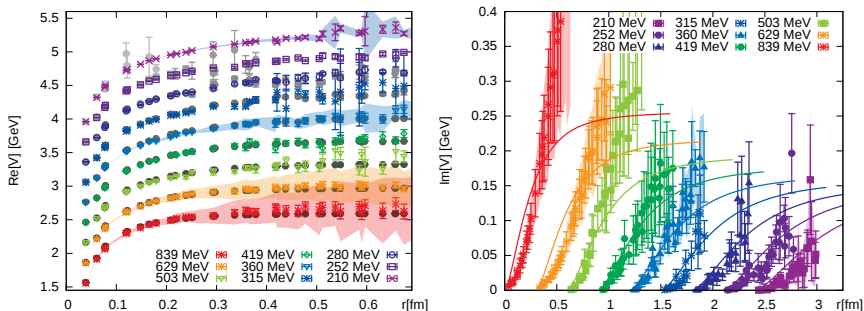


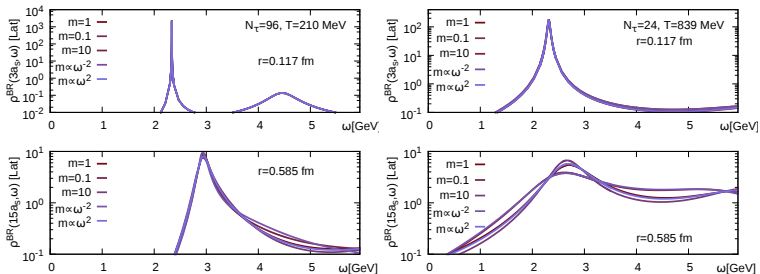
Figure: Lattice results for the potential at different temperatures and comparison to the free energies in Coulomb gauge (in grey).

Smooth transition between confining to Debye screened potential.

Spectrum: Dependence on the prior

We use different priors for the reconstruction

- Default: constant $m(\omega) = 1$, we check $m = 0.1, m = 10$.
- Change functional form $m(\omega) = \omega^2, \omega^{-2}$.

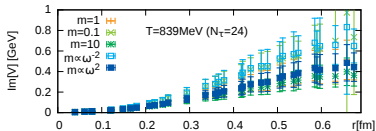
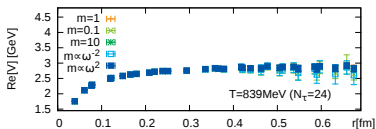
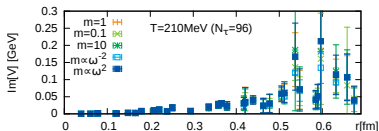
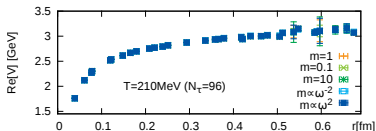


- Few changes, no systematic effect.
- Only large r and T are not so stable.

Potential: Dependence on the prior

We use different priors for the reconstruction

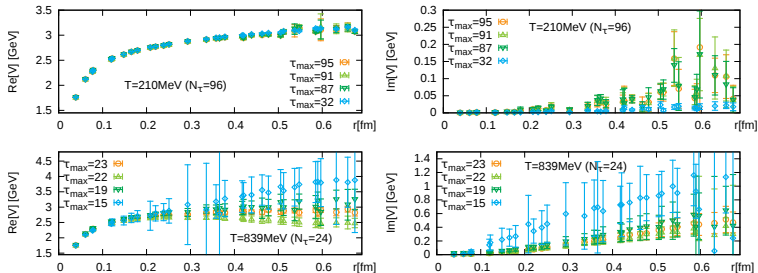
- Default: constant $m(\omega) = 1$, we check $m = 0.1, m = 10$.
- Change functional form $m(\omega) = \omega^2, \omega^{-2}$.



- Few changes, no systematic effect, jackknife error bars overlap.

Dependence on the number of data points

We vary the number of points used in the reconstruction:

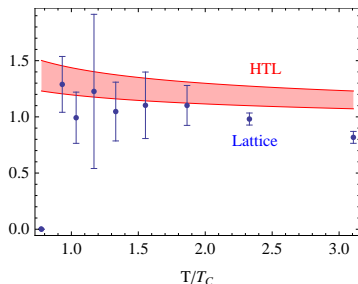
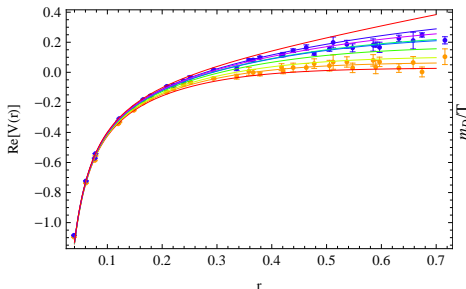


- Very stable except at high r and T .
- Jackknife error bars overlap.
- Is the T -dependence only due to the lower number of points?
- Taking the 32 first points from the $N_\tau = 96$ ($T=210\text{MeV}$) we can compare to $T=629$.

Debye masses (Preliminary)

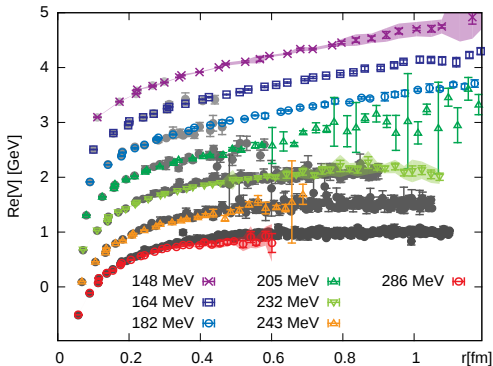
Debye-Hückel fit to the data enables a determination of the Debye mass [S. Dital, O. Kaczmarek, F. Karsch and H. Satz 2005]

$$\text{Re}[V](r, T) \equiv -\alpha \frac{e^{-m_D r}}{r} - \frac{\sigma}{2^{3/4} \Gamma(3/4)} \sqrt{\frac{r}{m_D}} K_{1/4}(m_D r) + c.$$



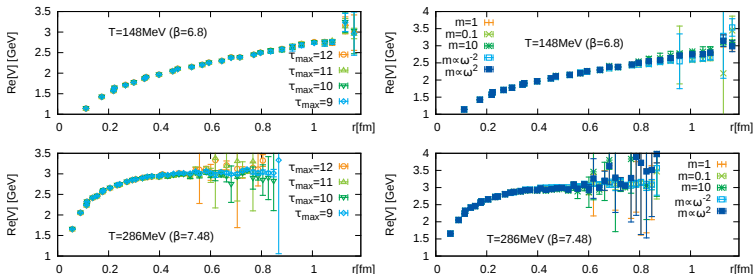
Temperature dependence of the potential: Dynamical Lattice

We used the $N_f = 2 + 1$ ASQTAD lattices with $m_l = m_s/20$ by the HotQCD collaboration, temperatures between $286\text{MeV} \geq T \geq 148\text{MeV}$ obtained varying the lattice spacing $\beta = 6.8 \dots 7.48$ at fixed $N_\tau = 12$.



Dependence on the number of data points and prior

We vary the number of points and the prior used in the reconstruction:



- Very stable except at high r and T .
- All the Jackknife error bars overlap!

Conclusion

We calculated the heavy quark potential from quenched lattice calculations:

- Main issue: reconstruct the spectrum from Euclidean data.
 - The extended MEM finds the potential peak but fails to capture its Lorentzian structure.
 - The new Bayesian approach captures the Lorentzian shape of the peak. We get the real part as well as the imaginary part in the case of precise data and large N_T .
- To extract the potential from the reconstructed spectra:
 - It is enough to fit the lowest peak
- Next:
 - Continuum limit on the lattice . . .
 - Check the charmonium and bottomonium spectrum!
 - Can we understand heavy ion collisions?

Test of the reconstructed spectra

Using **LO HTL perturbation theory** \rightarrow calculate $C_E(\tau, r)$, $C_>(t, r)$, $\rho(\omega, r)$, $\Phi(t, r)$, $V(r)$ and test the reconstruction method:

- MEM where we have chosen to give the exact Euclidean data.
- New BR method with relative gaussian errors in the data.

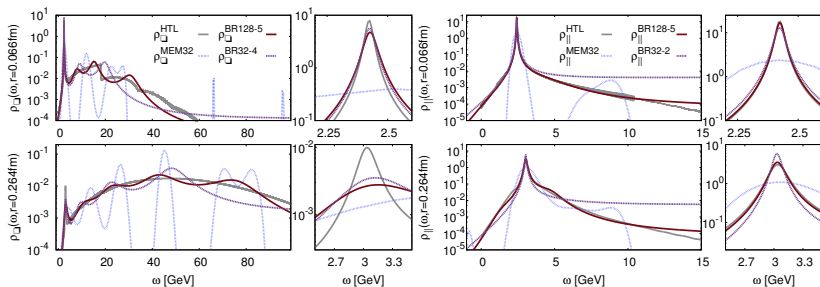
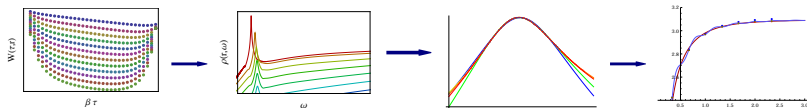


Figure: $r = 0.066 \text{ fm}$ (top) and $r = 0.264 \text{ fm}$ (bottom); two observables: Wilson loop (left); Wilson lines right).

Wilson loop harder to reconstruct because of cusp divergences

Test of the reconstructed potential

We can now fit the potential from the spectra for the HTL's and quenched lattice data:



We get:

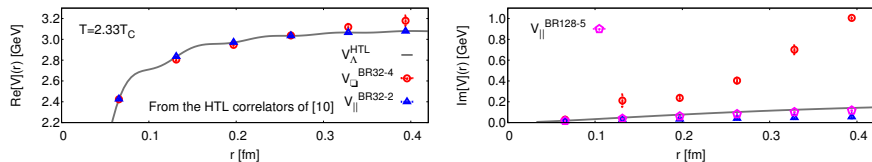


Figure: Reconstruction of the HTL ($T = 2.33T_C$) potential (solid line) based on the Euclidean HTL Wilson Loop $V_{\square}(r)$ (circle) and the HTL Wilson line correlator $V_{\parallel}(r)$ (triangle). (left): $\text{Re}[V](r)$ (right): $\text{Im}[V](R)$ requires $N_{\tau} = 128$ and 10^{-5} errors for a reliable determination

Temperature dependence of the potential: LO perturbation theory

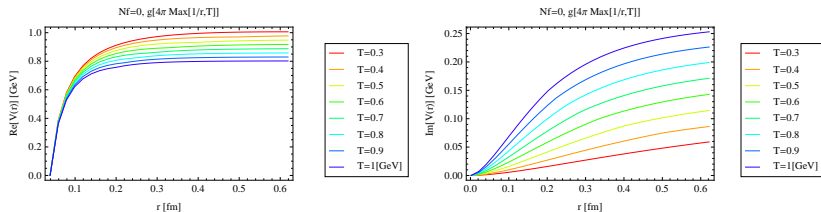


Figure: Lattice results and fits for the potential at different temperatures, (insert): fitted Debye masses [Digal et al 2005] together with HTL ($m_D = g(4\pi T)T$).

New Bayesian reconstruction method: Short summary

Inversion (10) \Leftrightarrow minimization procedure.

- Starting with some ρ_i 's, minimize the distance to the data

$$L = \frac{1}{2} \sum_{ij} (D_i - D_i^\rho) C_{ij} (D_j - D_j^\rho), \quad (11)$$

with C_{ij} the covariance matrix of the data.

- In because of errors the correct result should have $L \sim N_\tau$ so that

$$P(D|\rho) = \exp(-L - \gamma(L - N_\tau)^2) \quad (12)$$

and the limit $\gamma \rightarrow \infty$ is taken numerically.

Not yet enough to define a unique solution if $n_\omega > N_\tau \dots$

New Bayesian reconstruction method: Short summary

- Suppose that $\rho(\omega)$ is a **smooth function** that might be partly known (prior function $m(\omega)$).
- We encode this in a probability function for ρ itself:

$$P(\rho|m, \alpha) = \exp[S] = \exp \left[\alpha \sum_{l=0}^{n_\omega} \Delta\omega_l \left(1 - \frac{\rho_l}{m_l} - \log \frac{\rho_l}{m_l} \right) \right]. \quad (13)$$

- For any given $\alpha \rightarrow$ **unique solution** ω_l , $l = 0..n_\omega$ minimizing

$$P(\rho|D, m, \alpha) = \frac{P(D|\rho)P(\rho|m, \alpha)}{P(D|m, \alpha)}. \quad (14)$$

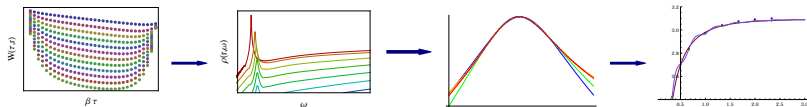
- The final result $P(\rho|D, m)$ is obtained by integrating out α

$$P(\rho|D, m) \propto P(D|\rho) \int d\alpha P(\rho|m, \alpha). \quad (15)$$

- Unlike for the MEM, we first **integrate over α explicitly** and then find the spectrum that minimize $P(\rho|D, m)$

From the Euclidean correlator to the potential

Summary of the full method:



- **Lattice computation:** Calculate the Wilson loop $W_{\square}(r, \tau)$ for all possible values of the imaginary time $\tau \in [0, \beta]$.
- **Analytic continuation:** extract the spectrum $\rho_{\square}(r, \omega)$ by inverting eq:

$$W_{\square}(r, \tau) = \int d\omega e^{-\omega\tau} \rho_{\square}(r, \omega).$$

- **Fit:** $V(r)$ can be extracted from the lowest peak of ρ .